Burn-up Characteristics and Criticality Effect of Impurities in the Graphite Structure of a Commercial-scale Prismatic HTGR

Y. Fukaya*, M. Goto, and T. Nishihara

HTGR Hydrogen and Heat Application Research Center

Japan Atomic Energy Agency (JAEA)

4002 Narita-cho, Oarai-machi, Higashiibaraki-gun, Ibaraki 319-1395, Japan

*E-mail: fukaya.yuji@jaea.go.jp

Phone: +81-29-267-1919 ex.3837

Fax: +81-29-266-7703

Total number of pages: 25

Total number of Tables: 5

Total number of Figures: 8

Abstract

This study investigates the burn-up characteristics and the criticality effect of impurities in the graphite structure of commercial-scale prismatic High Temperature Gas-cooled Reactor (HTGR), and thereby reconsiders the necessity of high-grade graphite material. In an HTGR, the core is filled with the graphite, and the impurities in the graphite have a non-negligible poison effect on the criticality. To account for the effect of the reflector blocks deployed adjacent to the fuel blocks, GTHTR300, commercial-scale HTGR, employed fine purified grade graphite material IG-110. Ideally, the fuel blocks should also employ IG-110; however, for economic purposes they are constructed from an un-purified grade graphite material IG-11. The poisoning effect of the impurity (which behaves like ^{10}B burn-up and is expressed in boron equivalents) decreases exponentially and eventually saturates at 1% of the initial boron equivalent. However, the reactivity worth of the fuel and reflector blocks with 0.03 ppm boron equivalents (equivalent to 1% of IG-11) is negligible (i.e., < 0.01%$\Delta k/kk'$). Because the poisoning effect of the impurity mimics that of naturally occurring boron, it was evaluated in whole-core burn-up calculations with the impurities represented by naturally occurring boron.

According to the results, the criticality of the commercial-scale HTGR is unaffected by the impurity levels (even in the un-purified grade IG-11) because the impurities burn cleanly until the End Of Cycle (EOC). Therefore, the economy of electricity generation by HTGRs can be improved by using the un-purified grade IG-11 instead of the fine purified grade graphite IG-110.

KEYWORDS: HTGR, graphite, impurity, burn-up characteristic

Highlight

・We evaluate the criticality effect of impurities in graphite block for HTGR by whole core burn-up calculations.

・We confirm the boron equivalent can be also employed for burn-up calculations.

・We conclude fine purified grade graphite IG-110 is not necessary from the viewpoint of criticality.

1. Introduction

The Japan Atomic Energy Agency (JAEA) has built a High Temperature Engineering Test Reactor (HTTR) (Saito, 1994), which is a prismatic-type High Temperature Gas-cooled Reactor (HTGR) that generates 30 MW thermal power. On the basis of the accumulated design, construction, and operational experience, JAEA has been conducting a design study of GTHTR300 series (Yan et al., 2003), it is a series of commercial-scale HTGRs with annular cores and thermal power outputs of 600 MW.

In the first experimental assessment of the HTTR, which was conducted by the fuel addition method at room temperature, the amount of fuel required for criticality has been predicted by many researchers; however, the amount was insufficient. In the core, dummy graphite blocks constructed from the un-purified grade graphite material IG-11 were replaced with fresh fuel blocks from the outer core region in the form of fuel columns. Other fuel and reflector blocks were constructed from the fine purified grade graphite material IG-110. The first criticality was achieved in an annular core comprising 19 fuel columns. However, in the simulation by using MVP (Nagaya et al., 2006), the first criticality was predicted in a core with 16 fuel columns (Nojiri et al., 1998). The MVP code simulates neutron transport by a Monte Carlo method (Nagaya et al., 2006).

After the experimental assessment, many researchers reevaluated the approach to criticality, which has now become a benchmark problem (IAEA, 2003). In one re-evaluation (Tanaka, 1999), the model was refined to achieve criticality in a core with 18 fuel columns;

however, one of the fuel column deviated from the experimental data. The researchers attributed this discrepancy to an underestimation of the impurity in IG-11. In this way, high-grade graphite is important for criticality, and employed in the core structure of GTHTR300 design.

The neutron capture cross-section of graphite is sufficiently low to achieve criticality even in Calder-Hall-type reactors (Centaur Communications Ltd, 1956), which are natural uranium fueled reactors. Therefore, the poisoning effect of the impurity is non-negligible. In the GTHTR300 design, where the criticality effect is regarded as important, the reflector blocks adjacent to the fuel blocks are constructed from the fine purified grade graphite IG-110. However, the fuel blocks, which should also employ IG-110, are constructed from the un-purified grade graphite IG-11 for economic purposes.

Furthermore, the burn-up characteristics of the impurity were not considered in the nuclear design. In the criticality calculations of GTHTR300, the poisoning effect is expressed in equivalents of unburnable boron, treating the impurity as a constant composition of naturally occurring boron. However, because the impurity is infinitely diluted by the graphite material, its criticality value (i.e., its boron equivalent (IAEA, 2002)) should be reduced by transmutation during burn-up without shielding effects. If sufficient impurity nuclides with large cross-sections are converted to nuclides with small cross-sections by End Of Cycle (EOC), the poisoning effect does not problematically affect the achievable burn-up and/or cycle length.

The present study investigates the necessity of employing IG-110 in commercial-scale HTGR from a criticality viewpoint. To this end, it evaluates the burn-up characteristics and criticality of impurity. Section 2 explains the core geometry of GTHTR300 and the calculation method. Section 3 investigates the burn-up characteristics of the impurity, which are necessary for evaluating the burnable impurity effect in the core calculations. In Section 4, the implications of the criticality effect for nuclear design are evaluated by whole-core burn-up calculations.

2. Calculation Method

2.1 Core geometry of GTHTR300 and calculation model

The major specifications (Nakata et al., 2003) of GTHTR300 are listed in Table 1. GTHTR300 is a commercial-scale HTGR design with a 600 MW thermal power output. Its annular core, which comprises two batches of fuel blocks, is packed with 14 wt% enriched uranium fuel. The cycle length is 730 days.

The core configuration is shown in Fig. 1. The fuel columns are composed of eight fuel block layers aligned in the axial direction. Each fuel block is approximately 1 m high, yielding an approximate core height of 8 m. Because of the axial arrangement of the GTHTR300 core parts, an axial fuel reloading is assumed. As the loading pattern for GTHTR300 design, JAEA devised and implemented a method called sandwich refueling (Yan et al., 2003). The fuel blocks are divided into irradiated and fresh fuel batches. The irradiated fuel blocks are sandwiched between the fresh fuel blocks, as shown in Fig. 2. In addition, the uranium inventory is slightly reduced from its original 7.09 t (Nakata et al., 2003), as the fuel structure was revised from the viewpoint of fuel fabrication (Fukaya et al., 2015). The target cycle length and average discharged burn-up are 730 days and 120 GWd/t, respectively.

To compare the criticality effect of the impurity, the core was divided into several parts as shown in Fig. 1. For the burn-up calculations in Section 4, the side reflectors and fuel blocks were divided into layers. The residence time of the reflector blocks is approximately 10 years (Sumita et al., 2003), However, to simplify the problem and obtain conservative results, the present study assumed that the reflectors were replaced at each refueling.

Table 1

Figs. 1and 2

2.2 Calculation method

In this study, the burn-up characteristics and criticality of impurity were assessed by core burn-up calculation implemented in MVP (Nagaya et al., 2006), a Monte Carlo neutron

transport code with evaluated nuclear data of JENDL-4.0 (Shibata et al., 2011). Moreover, the double heterogeneity of Coated Fuel Particles (CFPs) was directly analyzed using a statistical geometric model (Murata et al., 1997). The MVP calculations were implemented in three-dimensional whole-core models. The representative burn-up characteristics of the impurity and the detailed criticality effect (presented in Sections 3 and 4, respectively) were evaluated using two different models. The burn-up characteristics were determined by a one-batch core model, in which the whole fuel element was reloaded with fresh fuel without burn-up to generate libraries of ORIGEN code (Croff, 1983), and to determine the neutron flux level for the burn-up calculations. The criticality value of the impurity during operation, and the achievable cycle length, were evaluated using a two-batch core model with equilibrium cycles. To evaluate the impurity criticality effect accurately, the Burnable Poisons (BPs) and control rods were not modeled in these calculations.

The representative burn-up characteristics of the impurity were determined using the ORIGEN code as mentioned above. This code models the reactions of 394 nuclides. If transmutations of these nuclides are included, the number of activation products increases to 688. To generate the requisite library of one-energy group cross-sections (Fukaya et al., 2013), we condensed the 108-energy group infinite dilution cross-sections processed using the NJOY code (MacFarlane et al., 2010), with the neutron fluxes obtained by MVP calculations in the one-batch core model.

To prepare the cross-sections condensed by HTGR spectra for all activation products, multiple evaluated nuclear data libraries implemented in the NJOY code were employed. In order of descending priority, these libraries were JENDL-4.0 (Shibata et al., 2011) (311 nuclides), JEFF-3.1.2 (Koning et al., 2011a) (18 nuclides), JENDL/A-96 (Nakajima, 1991) (17 nuclides), JEFF-3.1/A (Koning et al., 2006) (30 nuclides), and TENDL-2011 (Koning et al., 2011b) (18 nuclides). JENDL-4.0 and JEFF-3.1.2 are the most reliable ones that can be utilize for criticality calculations. JENDL/A-96 and JEFF-3.1/A were prepared to cover activation products, which have many nuclides and are not so important for criticality.

TENDL-2011 covers the most number of nuclides because those are provided by the nuclear model for direct use basic physics, and those are less reliable compared with the evaluated nuclear data generated with experimental data such as JENDL-4.0 and JEFF-3.1.2.

2.3. Conversion method impurity to equivalent boron

The burn-up composition can be evaluated by ORIGEN code and the ORIGEN libraries generated in the manner described in Subsection 2.2. However, the burned impurity composition, which includes many nuclides, is difficult to take into account the poison effect to the core calculation by MVP. To perform this, extensive renovations would be necessary for code system of MVP, and it is not realistic. On the other hand, the reactivity worth of the impurity in the graphite is expressed by boron equivalent, which is weight fraction of equivalent naturally occurring boron, and has been treated as unburnable boron for core calculation as described in Section 1. The definition of the boron equivalent (IAEA, 2002) can be written as follows,

$$\mathrm{BE} = \sum_{i=1}^{n} \frac{\sigma_i}{\sigma_B} \frac{M_B}{M_i} w_i , \quad (1)$$

where,

BE: boron equivalent (ppm),

σ_B: microscopic thermal absorption cross-section for naturally occurring boron (cm^{-2}),

σ_i: microscopic thermal absorption cross-section for i-th nuclide(cm^{-2}),

M_B: atomic mass for naturally occurring boron (u),

M_i: atomic mass for i-th nuclide (u),

w_i: weight content for i-th nuclide (ppm).

As described in Eq. (1), to evaluate the boron equivalent, the mass fractions of impurities are converted to equivalent mass fraction for the naturally occurring boron with remaining the reactivity worth at the neutron energy of 0.025eV.

In this study, to obtain more accurate result, the definition of boron equivalent is evolved by using the condensed cross-sections for whole energy and reaction types of reactions in ORIGEN code as follows:

$$\mathrm{BE}' = \sum_{i=1}^{n} \frac{\sigma_{i(\mathrm{n},\gamma)} + \sigma_{i(\mathrm{n},\gamma)_\mathrm{e}} + \sigma_{i(n,\alpha)} + \sigma_{i(\mathrm{n,p})} - \sigma_{i(\mathrm{n,2n})} - \sigma_{i(\mathrm{n,2n})_\mathrm{e}} - 2\sigma_{i(\mathrm{n,3n})}}{\sigma_{B(\mathrm{n},\gamma)} + \sigma_{B(\mathrm{n},\gamma)_\mathrm{e}} + \sigma_{B(n,\alpha)} + \sigma_{B(\mathrm{n,p})} - \sigma_{B(\mathrm{n,2n})} - \sigma_{B(\mathrm{n,2n})_\mathrm{e}} - 2\sigma_{B(\mathrm{n,3n})}} \frac{\mathrm{M_B}}{\mathrm{M_i}} \mathrm{w_i}\,, \quad (2)$$

where,

BE': new boron equivalent proposed in this study (ppm),

$\sigma_{B(\mathrm{n},\gamma)}, \sigma_{i(\mathrm{n},\gamma)}$: microscopic radioactive capture cross-section for naturally occurring boron or i-th nuclide (cm^{-2}),

$\sigma_{B(\mathrm{n},\gamma)_\mathrm{e}}, \sigma_{i(\mathrm{n},\gamma)_\mathrm{e}}$: microscopic radioactive capture cross-section to an excited state of a daughter for naturally occurring boron or i-th nuclide (cm^{-2}),

$\sigma_{B(n,\alpha)}, \sigma_{i(n,\alpha)}$: microscopic cross-section of the (n,α) reaction for naturally occurring boron or i-th nuclide (cm^{-2}),

$\sigma_{B(\mathrm{n,p})}, \sigma_{i(\mathrm{n,p})}$: microscopic cross-section of the (n,p) reaction for naturally occurring boron or i-th nuclide (cm^{-2}),

$\sigma_{B(\mathrm{n,2n})}, \sigma_{i(\mathrm{n,2n})}$: microscopic cross-section of the (n,2n) reaction for naturally occurring boron or i-th nuclide (cm^{-2}),

$\sigma_{B(\mathrm{n,2n})_\mathrm{e}}, \sigma_{i(\mathrm{n,2n})_\mathrm{e}}$: microscopic cross-section of the (n,2n) reaction to an excited state of a daughter for naturally occurring boron or i-th nuclide (cm^{-2}),

$\sigma_{B(\mathrm{n,3n})}, \sigma_{i(\mathrm{n,3n})}$: microscopic cross-section of the (n,3n) reaction for naturally occurring boron or i-th nuclide (cm^{-2}).

In this study, the inventory of impurity is converted to boron equivalent using the relation in Eq. (2), and vice versa. If burn-up characteristics can also be represented by a few number of nuclides or a pseudo nuclide in the same manner as boron equivalent with the relation in Eq. (2), the poison effect can be easily taken into account to core calculations with

the burn-up characteristics.

Table 2

3.Calculation result and discussion

3.1 Verification of burn-up dependency of equivalent boron

In the context at Subsection 2.3, we verify compatibility of boron equivalent for burn-up calculation. Table 2 lists the composition of the IG-110 impurity (IAEA, 1993), determined in sample measurements and corrected for the nuclear design requirements of IG-11 and IG-110 in the present study. In a nuclear design requirement (Nakata, 2002), the boron equivalents of IG-11 and IG-110 were determined as 3 ppm and 0.5 ppm, respectively. The composition in Table 2 was normalized to match the boron equivalent, and used for this study.

The irradiation calculation of impurities with the compositions is performed by the ORIGEN code by using the library and the condition evaluated by MVP calculation assuming the one-batch core model for the fuel blocks and their adjacent reflector blocks (the inner and outer side reflectors, and the reflectors above and below the fuel; see Fig. 1). As shown in Fig. 3, the neutron flux was more heavily moderated in the reflector blocks than in the fuel blocks. The neutron flux levels were also evaluated using the MVP code and normalized by the thermal power of 600 MW. The calculated neutron fluxes in the fuel and reflector block were 1.07×10^{14} $cm^{-2}s^{-1}$ and 9.73×10^{13} $cm^{-2}s^{-1}$, respectively. Using the neutron flux levels, the burn-up characteristics of the fuel impurity were evaluated during the residence time of the fuel.

The results are presented in Fig. 4. The depression characteristics can be realized with any amount of impurity inventory as long as self-shielding effect, which reduces effective microscopic cross sections, does not work. Thus, the boron equivalents in the graph are normalized by the initial boron equivalents. The boron equivalent of the impurity decreases more rapidly in the reflector blocks than in the fuel blocks, because of the better neutron flux moderation. If the values fall below the boron equivalent ratio of IG-110 to IG-11 (0.17) within the EOC of one cycle (730 days), then IG-110 might not be necessary

from a criticality viewpoint. The boron equivalent of naturally occurring boron is also shown in Fig. 4. The boron equivalents of the impurity and naturally occurring boron essentially coincide, indicating that the impurity can be replaced by naturally occurring boron for determining the burn-up characteristics. Under this treatment, the poisoning effect of impurity burn-up is easily considered in the core criticality calculations. The boron equivalent ratios of the impurity elements were also evaluated in the fuel and reflector blocks, and are plotted in Figs. 5 and 6, respectively. Boron is the greatest contributor to the poisoning effect, followed by cobalt and lithium. The boron equivalent of boron decreased with increasing irradiation, and that of lithium decreased slightly. The boron equivalents of the other elements were approximately constant throughout the operation. More specifically, the boron equivalents of elements other than boron remained at approximately 1%. This suggests that, unlike the case of boron-only impurities, the boron equivalent is saturated at 1%. To evaluate the poisoning effect of this 1% boron equivalent, we performed criticality calculations by MVP code in the one-batch whole core model. The results are shown in Fig. 7. The lowest boron equivalent in the inventory (0.03 ppm, indicated by an arrow) corresponds to the 1% boron equivalent of IG-11. The reactivity worth is below 0.01% $\Delta k/kk'$ in both the fuel and reflector blocks, and can be ignored in the criticality calculations. To conclude, the burn-up characteristics of the impurity can be evaluated in terms of naturally occurring boron, thus simplifying the core calculations of the burning impurity. In addition, the boron equivalent curve shown in Fig.6 shows change in the tendency at the resident time 1000 days because of burning out of ^{10}B.

Figs. 3-7

3.2. Discussion of necessity of IG-110 from the result of whole core burn-up calculations

To confirm the necessity of IG-110, the cycle lengths of the equilibrium cycles were evaluated in core burn-up calculations under three impurity treatments. The first treatment was the conventional method, which employs IG-110 in the upper, lower and side reflectors,

and ignores irradiation depletion of the impurity. The second treatment similarly ignores impurity burn-up, but the all of the graphite material in the core structure employs IG-11. The third treatment represents the burn-up dependency of the impurity in terms of naturally occurring boron, and again constructs all of the graphite material from IG-11. The criticality throughout one equilibrium cycle is shown in Fig. 8. The cycle length was 28 days longer under the first treatment than under the second treatment (630 days versus 602 days). The average discharged burn-ups were 107.8 GWd/t and 103.0 GWd/t, respectively. On the basis of this result, IG-110 was deemed necessary in the previous study (Nakata et al., 2002). However, under the third treatment considered here, the cycle length was extended to 650 days, corresponding to a discharged burn-up of 111.2 GWd/t. This result suggests that the impurity in IG-11 burns up within one cycle. Table 3 shows the inventory ratio of ^{10}B to the initial inventory in each region during the EOC under the third treatment. The relative value can be regarded as the boron equivalent down to 1% (below this level, the criticality effect is negligible). The reflectors above and below the fuel are labeled as fuel blocks in this table. Almost all of the ^{10}B was incinerated within the first cycle in Layers 1, 3, 5 and 7 (which constitute the first batch). The ^{10}B in the reflector region was also clearly incinerated at the EOC. In the previous study, IG-11 was employed in the fuel blocks for economic reasons. Consequently, the cycle length was longer in the third case than in the second case. It is concluded that IG-110 need not be employed, because the poisoning effect was depleted during burn-up. Moreover, the use of the cheaper material IG-11 would reduce the cost of electricity generation. In addition, the poisoning effect of the impurity can be compensated by changing the BP rod design.

Table 3 and Fig. 8

3.4 Reactor safety and graphite material

In the present study, the criticality effect of impurities in graphite material, *that is*, “boron equivalent”, is discussed. On the other hand, there is another index of impurities in graphite material, *that is*, “ash concentration”. In this section, the graphite material and reactor

safety are discussed. In general, the graphite with higher ash concentration shows lower material performance. For example, IG-11 shows more oxidation reaction than IG-110. (Kawakami, 1986) However, the integrity as reactor stricture and reactor safety depend on safety design. As shown in Fig. 1, IG-11 are employed for the most part of blocks. (Nakata et al., 2002, Nakata et al., 2003) The center reflector block of 45 columns and fuel block of 90 columns employ IG-11, and the inner side reflector block of 30 columns and outer side reflector block of 45 columns employ IG-110. In the standard design, fuel block, which has complex geometry and needs mechanical strength compared with reflector block, also employs IG-11. For the graphite integrity and reactor safety, safety evaluation on the depressurized accident (Katanishi et al., 2007), where air ingress and graphite oxidation occur, was performed. In the accident, the inner and outer pipes of coaxial double piping for helium flow simultaneously break. After the loss of coolant helium gas, air in the reactor building enters the inside of the primary system from ruptured opening of piping. The reactor building works as confinement. The replace of air from environment and internal gas is limited by the leak rate of the reactor building. For the integrity graphite structure, the integrity of graphite support plate for fuel rod of fuel block was discussed from the calculated oxidation distribution in the reactor core under the circumstance. The maximum equivalent decrease of thickness of support plate was calculated to be 1.9 mm, while criteria to maintain the integrity of fuel support was 2 mm in each surface. It was clarified that structural integrity of fuel support can be maintained even in case of air ingress by depressurization accident and the coolable geometry of fuel rod can be kept. The research (Katanishi et al., 2007) concluded that the recriticality of reactor core by degradation of fuel structure by oxidation would not occur in this accident. The oxidation of reflector block is not regard as problematic in the safety evaluation. Replacing the all IG-110 blocks to IG-11 is also feasible.

4. Conclusions

In GTHTR300 (a commercial-scale HTGR), a fine purified grade IG-110 graphite

material was used to ensure criticality. In the present study, the necessity of this expensive material was reconsidered by evaluating the burn-up characteristics of the impurity contained in it and the criticality effect. First, the characteristics were evaluated in whole-core MVP calculations using the one-batch model and in burn-up calculations using the ORIGEN code. The impurity exhibited the following characteristics:

- Boron made a far greater contribution to the poisoning effect than the other impurity elements.
- The burn-up characteristics of criticality could be represented by naturally occurring boron. The characteristics were saturated at 1% boron equivalent, at which point the poisoning effects of all impurities except boron were constant.
- Assuming the use of IG-11 for both fuel and reflectors, the saturated boron equivalent level was 0.03 ppm, indicating a negligible criticality effect.

These results indicate that the burn-up characteristics of the impurity can be evaluated in a straightforward manner by representation using naturally occurring boron. In order to evaluate the necessity of using IG-110 in GTHTR300, the burn-up characteristics were evaluated in whole-core burn-up calculations implemented in the MVP code with equilibrium cycles. The case with IG-11 extended the cycle length over that of the conventional design approach using IG-110 by taking the impurity burn-up into account. Moreover, to reduce costs, IG-11 is already employed in the fuel blocks of conventional GTHTR300. The burn-up characteristics confirmed that the impurity was sufficiently depleted at the EOC. Therefore, IG-110 appears to be unnecessary from the viewpoint of criticality also for the reflector blocks, and cheaper electricity generation can be realized by replacing IG-110 with cheaper IG-11.

Acknowledgements

Authors appreciate Dr. J. Sumita of JAEA who gives insightful comments for graphite material, and Dr. Y. Nagaya of JAEA who supports to use MVP code. Authors also

appreciate Dr. S. Nakagawa of JAEA who is the specialist of safety analysis and support to write the Section 3.4.

References

Centaur Communications Ltd, 1956. Calder Hall Power Station. The Engineer. 5, 466-468.

Croff, A. G., 1983. ORIGEN2: A Versatile Computer Code for Calculating the Nuclide Compositions and Characteristics of Nuclear Material. Nucl. Technol. 62, 335-352.

Fukaya, Y., Ueta, S., Goto, M., et al., 2013. Study on methodology to estimate isotope generation and depletion for core design of HTGR. JAEA-Research 2013-035, Japan Atomic Energy Agency. (in Japanese)

Fukaya, Y., Goto, M., Nishihara, T., 2015. Development on nuclear design model for detailed design of clean burn HTGR. JAEA-Technology 2015-017, Japan Atomic Energy Agency (in Japanese)

IAEA, 1993. The status of graphite development for gas cooled reactors. IAEA-TECDOC-690, International Atomic Energy Agency.

IAEA, 2002. Guidelines for nuclear transfers. INFCIRC/254/Rev.5/Part 1, International Atomic Energy Agency.

IAEA, 2003. Evaluation of High Temperature Gas Cooled Reactor Performance: Benchmark Analysis Related to Initial Testing of the HTTR and HTR-10. IAEA-TECDOC-1382, International Atomic Energy Agency.

Katanishi, S., Kunitomi, K., 2007. Safety evaluation on the depressurization accident in the gas turbine high temperature reactor (GTHTR300). Nucl. Eng. Des., 237, 1372-1380.

Kawakami, H., 1986. Air oxidation behavior of carbon and graphite materials for HTGR. Tanso, 124, 26–33.

Koning, A. J., Forrest, R., Kellett, M., et al., 2006. The JEFF-3.1 Nuclear Data Library. JEFF Report 21, Nuclear Energy Agency, Organization for Economic Co-operation and Development.

Koning, A. J., Bauge, E., Dean, C. J., et al., 2011a. Status of the JEFF Nuclear Data Library.

J. Korean Phys. Soc., 59 (2),1057-1062.

Koning, A. J., Rochman, D., 2011b. TENDL-2011:TALYS-based Evaluated Nuclear Data Library. (URL:http://www.talys.eu/)

MacFarlane, R. E., Kahler, A. C., 2010. Methods for Processing ENDF/B-VII with NJOY. Nucl. Data Sheets, 111, 2739-2890.

Murata, I., Takahashi, A., Mori, T., et al., 1997. New Sampling Method on Continuous Energy Monte Carlo Calculation for Pebble Bed Reactors. J. Nucl. Sci. Technol. 24, 734-744.

Nagaya, Y., Okumura K., Mori, T., 2006. A Monte Carlo neutron/photon transport code MVP 2. *Trans. Am. Nucl. Soc.* 95, 662-663.

Nakajima, Y., 1991. JNDC WG on Activation Cross Section Data: JENDL Activation Cross Section File. Proc. the 1990 Symposium on Nuclear Data, JAERI-M 91-032, Japan Atomic Energy Research Institute, 43-57.

Nakata, T., Katanisi, S., Takada, S., et al., 2002. Nuclear Design of the Gas Turbine High Temperature Reactor (GTHTR300) (Contract Research). JAERI-Tech 2002-066, Japan Atomic Energy Research Institute. (in Japanese)

Nakata, T., Katanishi, S., Takada, S., et al., 2003. Nuclear, Thermal and Hydraulic Design for Gas Turbine High Temperature Reactor (GTHTR300). J. At. Energy Soc. Jpn. 2, 478-489. (in Japanese)

Nojiri, N., Nakano, M., Ando, H., et al., 1998. Preliminary Analyses for HTTR's Start-up Physics Tests by Monte Carlo Code MVP. JAERI-Tech 98-032, Japan Atomic Energy Research Institute. (in Japanese)

Saito, S., Tanaka, T., Sudo, Y., et al., 1994. Design of high temperature engineering test reactor (HTTR). JAERI 133, Japan Atomic Energy Research Institute.

Shibata, K., Iwamoto, O., Nakagawa, T., et al. 2011. JENDL-4.0: A New Library for Nuclear Science and Engineering. J. Nucl. Sci. Technol., 48 1-30.

Sumita, J., Ueta, S., Kunitomi, K., et al., 2003. Reprocessing Technologies of the High

Temperature Gas-Cooled Reactor (HTGR) Fuel. J. At. Energy Soc. Jpn. 2, 546-554. (in Japanese)

Tanaka, T., 1999. Critical Experiment of HTTR. Nuclear Data News. 63. (in Japanese)

Yan, X., Kunitomi, K., Nakata, T., Shiozawa, S., 2003. GTHTR300 design and development. Nucl. Eng. Des. 222, 247-262.

Table captions

Table 1 Major specifications of GTHTR300

Table 2 Impurity composition of IG-110

Table 3 Inventory ratio of ^{10}B to initial inventory at the EOC

Figure captions

Fig. 1 Core geometry of GTHTR300

Fig. 2 Sandwich refueling scheme

Fig. 3 Neutron fluxes in fuel blocks and reflector blocks

Fig. 4 Burn-up trends of impurity and naturally occurring boron in the fuel and reflector blocks

Fig. 5 Burn-up trends of the various elements in the fuel blocks

Fig. 6 Burn-up trends of the various elements in the reflector blocks

Fig. 7 Dependency of poisoning effect on boron inventory

Fig. 8 Criticality trends under different impurity treatments

Table 1 Major specifications of GTHTR300

Item	Value
Thermal power (MWt)	600
Electric generation (MWe)	
Gross:	280
Net:	274
Uranium inventory (ton)	7.01
^{235}U enrichment (wt%)	14.0
Cycle length (days)	730
Number of batch	2
Discharge burn-up (GWd/t)	120

Y. Fukaya:

Burn-up Characteristics and Criticality Effect of Impurity Contained into Graphite Structure for Commercial Scale Prismatic HTGR

Table 2 Impurity composition of IG-110

Element	Inventory (ppm)
Li	0.002
B	0.02
Na	0.05
Mg	0.006
Al	0.06
Ca	0.08
K	0.03
Ti	0.006
V	0.018
Cr	0.006
Fe	0.06
Mn	0.004
Co	0.014
Ni	0.006
Cu	0.05
Zn	0.06

Table 3 Inventory ratio of ^{10}B to initial inventory at the EOC

	Fuel block	Inner side ref.	Outer side ref.
Top ref. layer	3.29×10^{-2}	-	-
1st layer	1.35×10^{-2}	1.29×10^{-3}	8.98×10^{-5}
2nd layer	9.55×10^{-5}	5.29×10^{-4}	1.30×10^{-5}
3rd layer	5.86×10^{-3}	2.22×10^{-4}	1.10×10^{-5}
4th layer	5.00×10^{-5}	4.83×10^{-4}	1.72×10^{-5}
5th layer	7.21×10^{-3}	3.49×10^{-4}	1.14×10^{-5}
6th layer	6.92×10^{-5}	1.25×10^{-2}	6.72×10^{-4}
7th layer	1.20×10^{-2}	8.60×10^{-4}	4.53×10^{-5}
8th layer	9.20×10^{-4}	1.62×10^{-2}	2.51×10^{-3}
Bottom ref. layer	1.86×10^{-1}	-	-

Y. Fukaya:

Burn-up Characteristics and Criticality Effect of Impurity Contained into Graphite Structure for Commercial Scale Prismatic HTGR

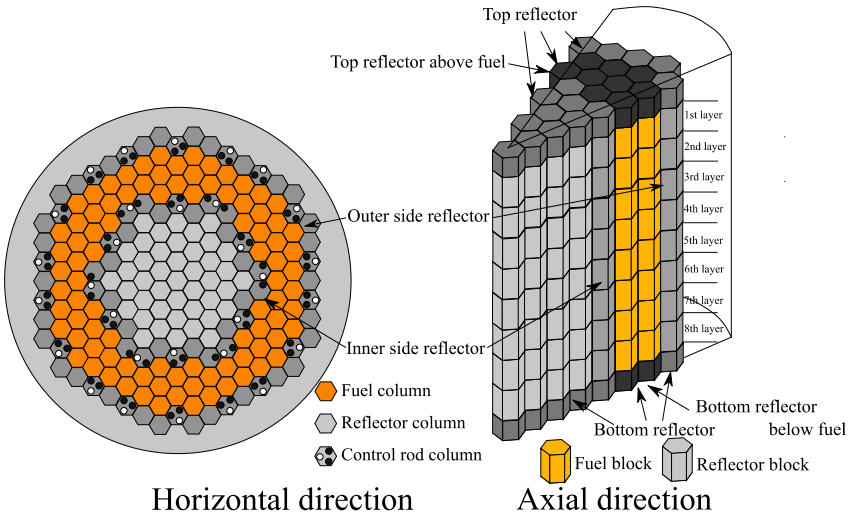

Fig. 1 Core geometry of GTHTR300

Y. Fukaya:

Burn-up Characteristics and Criticality Effect of Impurity Contained into Graphite Structure for Commercial Scale Prismatic HTGR

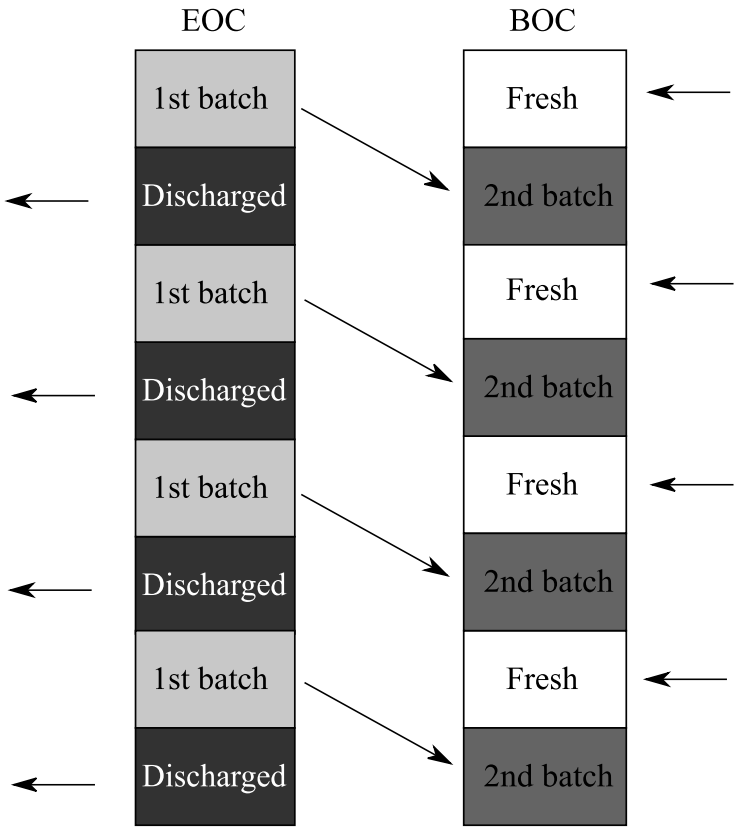

Fig. 2 Sandwich refueling scheme

for Commercial Scale Prismatic HTGR

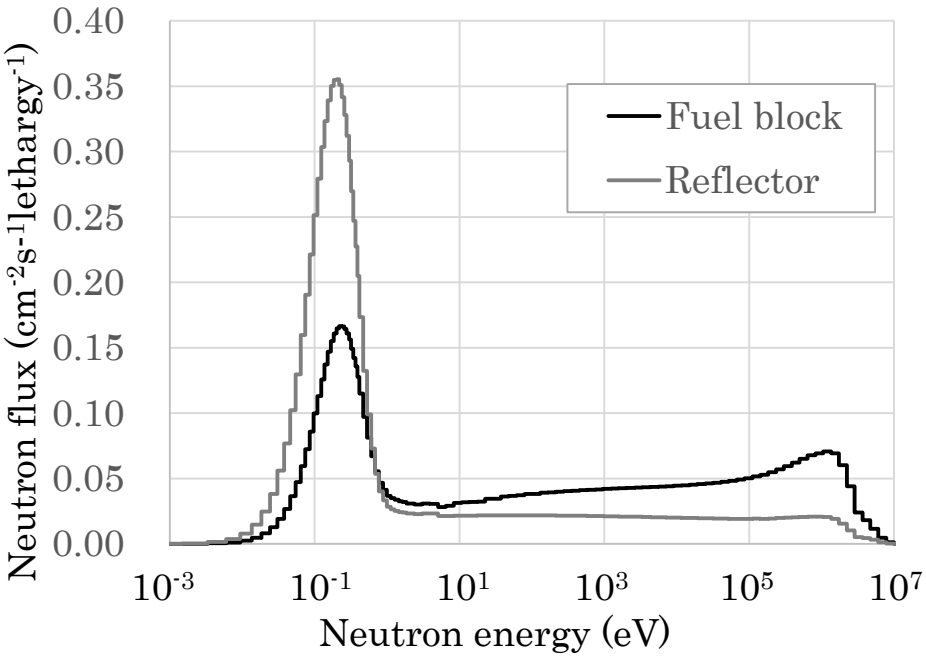

Fig. 3 Neutron fluxes in the fuel and reflector blocks

Y. Fukaya:

Burn-up Characteristics and Criticality Effect of Impurity Contained into Graphite Structure for Commercial Scale Prismatic HTGR

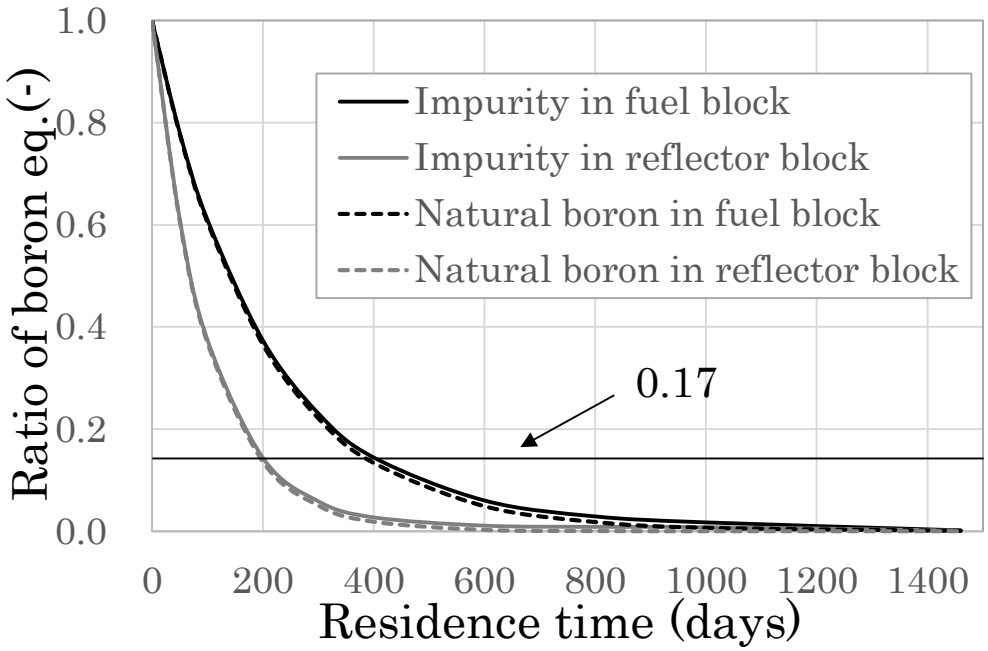

Fig. 4 Burn-up trends of impurity and naturally occurring boron in the fuel and reflector blocks

Y. Fukaya:

Burn-up Characteristics and Criticality Effect of Impurity Contained into Graphite Structure for Commercial Scale Prismatic HTGR

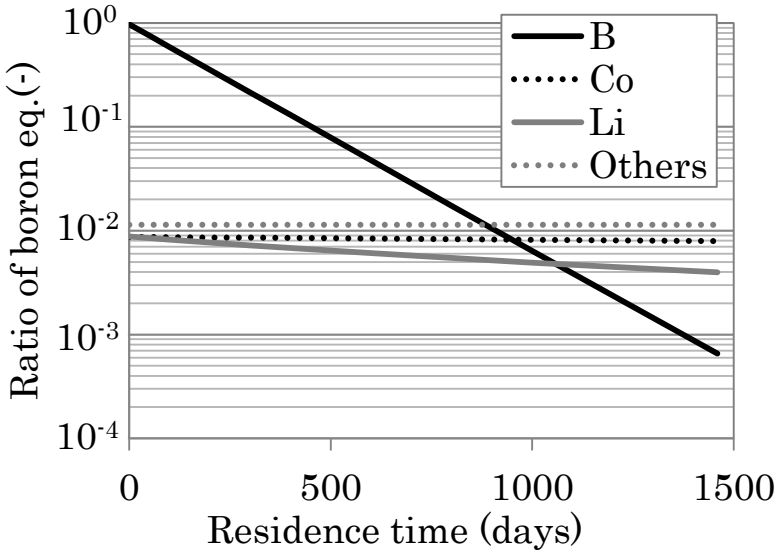

Fig. 5 Burn-up trends of the various elements in the fuel blocks

Y. Fukaya:

Burn-up Characteristics and Criticality Effect of Impurity Contained into Graphite Structure for Commercial Scale Prismatic HTGR

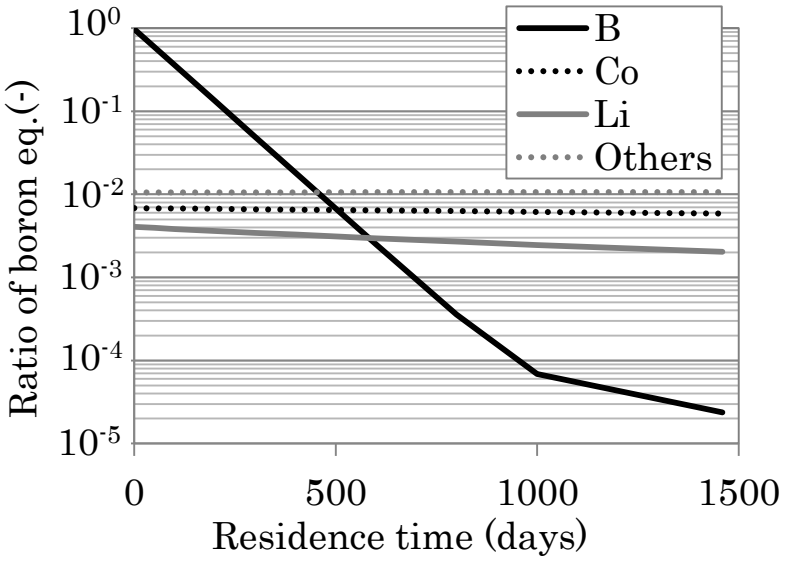

Fig. 6 Burn-up dependency of the various elements in the reflector blocks

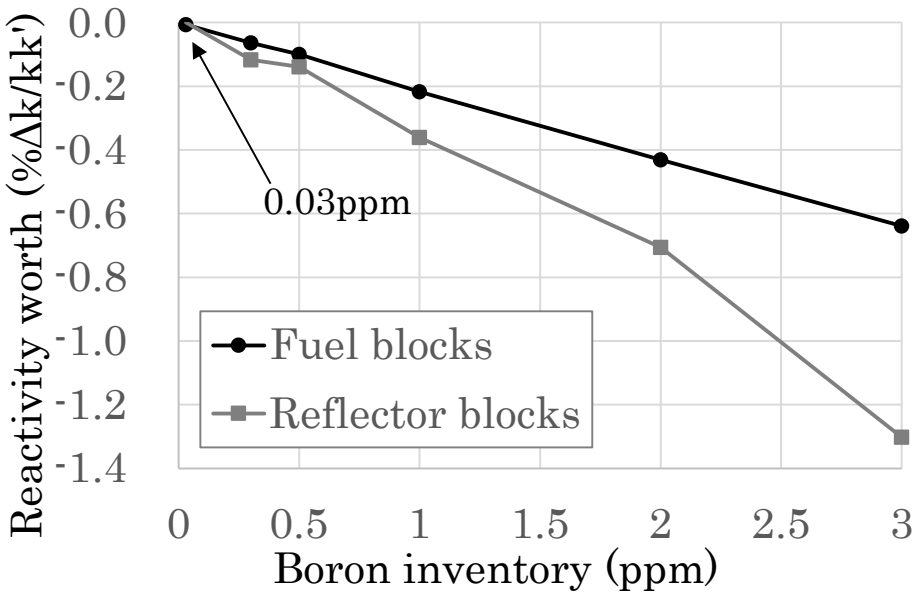

*Statistical error is negligible.

Fig. 7 Dependency of poisoning effect on boron inventory

Y. Fukaya:

Burn-up Characteristics and Criticality Effect of Impurity Contained into Graphite Structure for Commercial Scale Prismatic HTGR

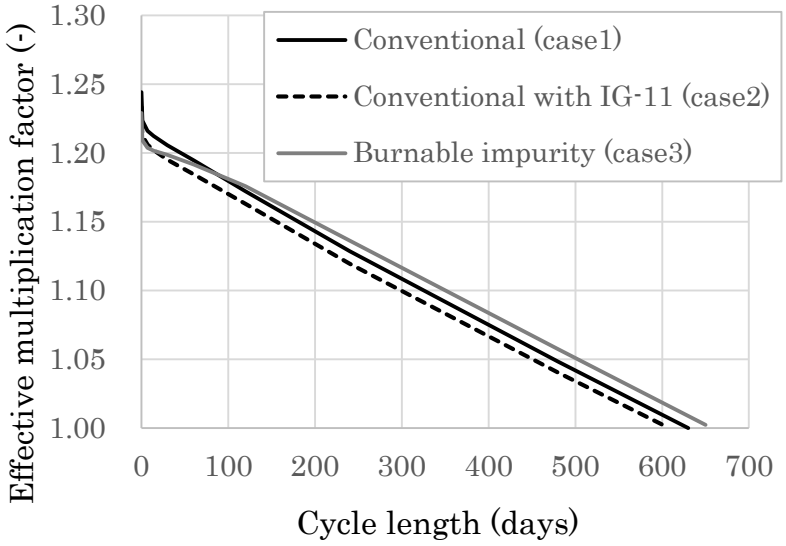

*Statistical error is negligible.

Fig. 8　Criticality trends under different impurity treatments

Y. Fukaya:

Burn-up Characteristics and Criticality Effect of Impurity Contained into Graphite Structure for Commercial Scale Prismatic HTGR